Pramāṇa, Vol. 2, No. 5, 1974, pp 259–268. Printed in India.

Shape mixing as an approximation to shell model ^{24}Ne

S B KHADKIKAR, D R KULKARNI and S P PANDYA
Physical Research Laboratory, Ahmedabad 380009

MS received 4 February 1974; after revisior 5 April 1974

Abstract. Band mixing calculations have been done for ^{24}Ne including the two degenerate prolate and oblate Hartree-Fock states and also some particle-hole excited states in the projection formalism using an interaction obtained by Preedom and Wildenthal. The energy spectrum agrees very well with the experimental results as well as the exact shell model calculations. Thus the band mixing calculations provide a good approximation to the lengthy exact shell-model calculations. In addition they offer a physical insight into the collective nature of the nucleus as nuclear states are described in terms of only a few 'intrinsic' states.

Keywords. Band mixing, energy spectrum, E2 transition probabilities, ^{24}Ne.

1. Introduction

The extensive configuration mixing calculations (Halbert *et al* 1971) performed in the framework of shell model indicate that the properties of several nuclei in the beginning of the d–s shell region are well described in this formalism. However the exact shell model calculations become prohibitively large as the number of valence nucleons outside the inert core (^{16}O in this case) increases. As a result, most of the shell model calculations have to be carried out in a suitably truncated space. The criteria for truncation are generally such as to exclude the configurations which are well above a suitably defined energy of interest. The energy of a particular configuration, in practice, is estimated on the basis of single particle energies to be used in a given calculation. Even such truncation schemes, besides introducing some error, do not always make the computations compact enough to be tackled easily. One therefore looks for some alternative formalism which is computationally simpler and yet yields to a good approximation the shell model results.

It is well known that the projected Hartree-Fock (PHF) formalism offers in general a good approximation to the shell model configuration mixing calculations, and describes well the states belonging to the ground band. However, where the HF gaps are found to be small, *e.g.*, in ^{24}Mg, one has to either invoke band mixing procedures or consider more complicated shapes such as a triaxial one. Also in nuclei in upper d–s shell ($28 \leqslant A \leqslant 40$), the Hartree-Fock calculations have not been very successful in predicting shapes, perhaps because of dominant pairing effects and small HF gaps in such calculations. It is therefore natural to attempt to extend the same formalism to explain other low-lying excited states not belonging to the ground band. The extension of this formalism consists of using several

different HF states and states obtained by particle-hole excitations from them as intrinsic states. The good angular momentum states, projected from these determinantal states, can be used as a basis for constructing and diagonalizing the Hamiltonian matrix. Since in general the states of the same angular momentum projected from different intrinsic states are not orthogonal, it becomes necessary to form orthogonal sets of vectors before proceeding to diagonalization. The truncation scheme to be followed in such a calculation is based on the intrinsic excitation energies of Hartree-Fock configurations, rather than the single particle energies relative to the core. Since the basis states are derived in a self-consistent manner from the two-body interaction to be used in the calculations, it is expected that relatively few configurations will suffice to reproduce the results of shell model calculations. In addition, even the truncation criteria in this scheme are directly based on the nature of the two-body interaction. A few such band mixing calculations have been reported earlier in the literature (Macfarlane and Shukla 1971). Besides simplifying the computations, the band mixing calculations enable us to describe the low-lying states in terms of only a few intrinsic states. In other words, the structure of these states can be analysed and physically visualised in terms of these intrinsic states. Such analysis in turn is likely to throw valuable light on the underlying collective nature of the states and their interrelationships. This aspect of the band mixing calculations is important, since in the shell-model calculations such analysis is not possible as the collectivity of a state results from a large amount of configuration mixing.

In this paper we report the band mixing calculations for ^{24}Ne. The energy spectrum and the electric transition probabilities thus obtained are compared with available experimental results (Howard *et al* 1970, Becker *et al* 1968) as well as the results of the shell model calculations of Robertson and Wildenthal (1973). We show that a close agreement with the shell model spectrum can be achieved by using as few as seven determinantal states.

Earlier Khadkikar *et al* (1971) have reported preliminary calculations on ^{24}Ne in which they have included the lowest oblate and the lowest prolate HF states along with some important $K = 0$ states obtained by particle-hole excitations over them. They used the renormalised two-body matrix elements of Kuo (1967). Though they could not get a good agreement with the observed level scheme, they showed that the apparent lack of rotational features of ^{24}Ne is understandable qualitatively, as arising from the mixing of different bands. We present here the results of more complete calculations which include additional $K = 2$ bands and use an interaction which we feel is better suited for this region. The fact that our calculated spectra agree well both with the shell model as well as the experimental spectra is due partly to the inclusion of the $K = 2$ bands and partly to the nature of two-body interaction used in these calculations.

2. Band mixing calculations

We have used the two-body matrix elements obtained by Preedom and Wildenthal (1972, hereafter referred to as PW interaction) along with the experimental single particle energies of ^{17}O: $\epsilon_{d_{5/2}} = 0$ MeV, $\epsilon_{d_{3/2}} = 5{\cdot}08$ MeV and $\epsilon_{s_{1/2}} = 0{\cdot}87$ MeV, to generate the Hartree-Fock intrinsic states. The two-body matrix elements of

PW interaction were obtained essentially by modifying the renormalized interaction of Kuo (1967) in the following way. The 16 matrix elements which involve only the $d_{5/2}$ and $s_{1/2}$ states were treated as free and independent parameters. The remaining 47 matrix elements of the Kuo interaction were altered with the prescription

$$\langle j_1 j_2 JT \mid H \mid j_3 j_4 JT \rangle = A_1 \langle j_1 j_2 \mid H \mid j_3 j_4 \rangle_{\text{Kuo}} + A_2 \delta_{j_1 j_3} \delta_{j_2 j_4}$$

The 16 independent matrix elements and the constants A_1 and A_2 were then varied to obtain the best possible fit to the selected set of observed energy levels of the nuclei with $A = 18$ to 22.

The lowest oblate and prolate Hartree-Fock (HF) intrinsic states, obtained for the nucleus ^{24}Ne, are found to be almost degenerate. It may be noted that this nucleus has the time-reversal symmetry but no neutron-proton (isospin) symmetry and therefore the neutron and proton HF orbitals are different. Implications of this are discussed later. Tables 1 and 2 give the components of the proton and neutron single particle orbitals of the oblate and prolate HF solutions respectively. The energies of the deformed single particle proton and neutron states are shown in figure 1 for both the HF solutions. It can be seen that for the oblate solutions the proton gap is smaller than the neutron gap, whereas for the prolate solution the neutron gap is smaller than the proton gap.

As described earlier, in the band mixing calculations one includes several determinantal states. In our calculations we have considered the lowest prolate and the oblate HF states along with other intrinsic states obtained as follows. The lowest prolate and the oblate HF states are obtained by occupying the corres-

Table 1. Structure of the neutron and proton orbitals for oblate HF solution of ^{24}Ne is given. The upper numbers correspond to protons and the lower ones to neutrons. The rest of the orbitals are related to these by time reversal.

k	$s_{1/2}$	$d_{3/2}$	$d_{5/2}$
5/2	0	0	1·0
	0	0	1·0
3/2	0	0·5030	0·8643
		0·4611	0·8874
1/2	0·5528	−0·1227	0·8242
	0·5508	−0·0992	0·8287
1/2′	0·7125	−0·4432	−0·5439
	0·7636	−0·3407	−0·5484
3/2′	0	−0·8643	0·5030
	0	−0·8874	0·4610
1/2″	0·4320	0·8880	−0·1575
	0·3368	0·9349	−0·1119

Table 2. Structure of the proton and neutron orbitals for prolate HF solution of ^{24}Ne is given. The upper numbers correspond to protons and the lower ones to neutrons. The rest of the orbitals are related to these by time reversal.

k	$s_{1/2}$	$d_{3/2}$	$d_{5/2}$
1/2	−0·3195	−0·2805	0·9051
	−0·3593	−0·3184	0·8772
3/2	0	−0·1317	0·9913
	0	−0·1224	0·9925
5/2	0	0	1·0
	0	0	1·0
1/2′	0·5039	0·7586	0·4130
	0·6658	0·5712	0·4800
1/2″	0·8025	−0·5880	0·1010
	0·6539	0·7565	−0·0068
3/2′	0	0·9913	0·1317
		0·9925	0·1224

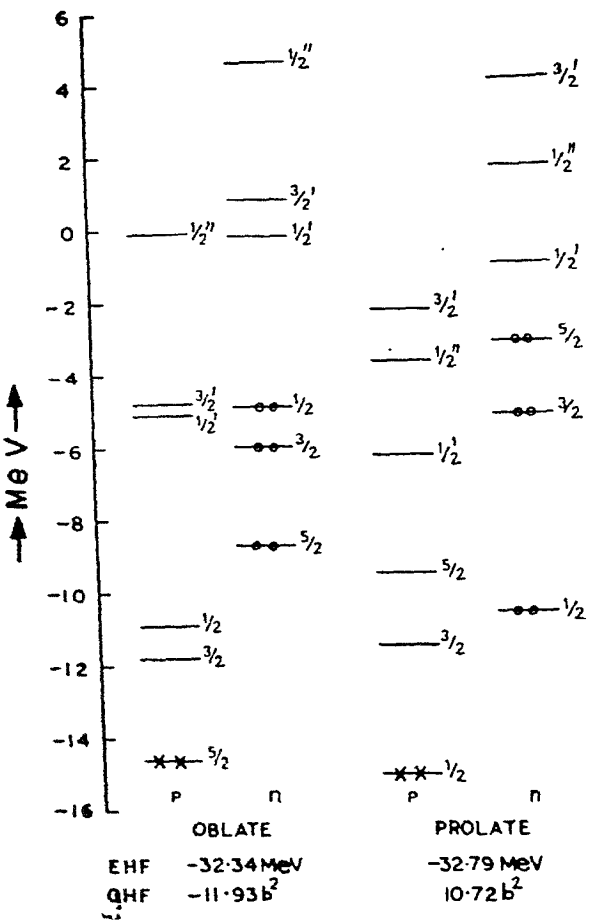

Figure 1. The energies, the quadrupole moments and the single particle spectra of the oblate and the prolate HF states of ^{24}Ne.

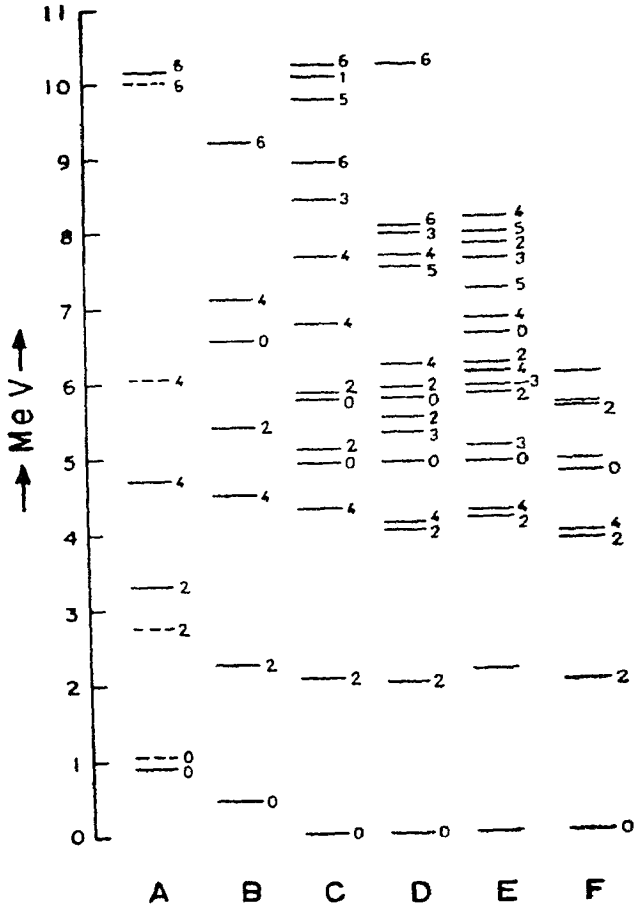

Figure 2. The energy spectra of ^{24}Ne. (A) the energy levels projected from the prolate HF state (solid lines) and the oblate HF state (dashed lines); (B) the spectrum obtained by mixing the levels given in part A; (C) the spectrum obtained by mixing the states projected from all K = 0 bands; (D) the final spectrum obtained by mixing the states projected from all K = 0 and two K = 2 bands (6 and 7 in table 3); (E) the shell model spectrum; and (F) the experimental spectrum.

ponding lowest single particle HF orbitals (*see* figure 1). It may be noted that due to time-reversal symmetry each HF single particle orbital can accommodate only two particles. The prolate solution therefore consists of two protons in the orbital k = 1/2 and six neutrons in the orbital k = 1/2, 3/2 and 5/2. On the other hand, in the lowest oblate solution, the two protons occupy the orbital k = 5/2 and the six neutrons occupy the orbitals k = 5/2, 3/2 and 1/2. These occupied orbitals as well as the excited unoccupied orbitals are shown in figure 1. Other intrinsic states formed using the same single particle level schemes will obviously contain some excited unoccupied orbitals and therefore will lie higher in energy than the corresponding lowest state. In practice the occupancy of these excited single particle orbitals in the intrinsic states will be an approximate measure of how high they will lie in energy from the lowest state. Also the difference in

occupancy of single particle orbitals in the excited intrinsic state from that of the lowest state is used to classify these states. For example, the intrinsic states in which only one particle goes to the unoccupied excited orbital while all others are in the lowest orbitals are known as one particle-one hole excited states and so on. In other words, the excited intrinsic states in the HF framework are the particle-hole excited states from the lowest HF states.

Several additional determinantal states obtained by one particle-one hole (1p–1h) and two particle—two hole (2p–2h) excitations over the oblate and the prolate HF intrinsic states are included in the present calculations. The determinantal states which lie more than 7 MeV above the lowest states are however neglected. Table 3 gives the structure and intrinsic energies of nine determinantal states used in the calculations. It may be noted that the calculation now includes five $K = 0$ bands and four $K = 2$ bands.

The next phase of the calculations consists of projecting the states of good angular momenta from the various intrinsic states. Since these basis states are in general not orthogonal, a set of orthonormal vectors is obtained by diagonalizing the overlap matrix for each angular momentum state separately. From this orthonormal basis, a Hamiltonian matrix is formed and diagonalized to obtain the energies and wave functions of different states.

It is worth noting that with our choice of particle-hole excitations near the Fermi surfaces of protons and neutrons the intrinsic states so obtained (table 3) would have exact isospin only if there was perfect proton-neutron symmetry. However this symmetry is somewhat broken here as seen from tables of the orbitals (tables 1 and 2). So one would like to ascertain the extent of the admixture of different isospin values in these states. For the nucleus ^{24}Ne containing 10 protons and 14 neutrons, the value of total isospin projection T_z is 2. It means that this nucleus can have states of good isospin values $T = 2$ and higher. We have therefore projected the states of isospin values $T = 2$, 3 and 4 from all the intrinsic states used in the calculations. We have found that the largest admixture of isospin values other than $T = 2$ was only 0·1%. One therefore expects that this small isospin mixing is negligible, and will not affect the calculated spectrum appreciably.

Besides the energies, we have also calculated the quadrupole moments and electric transition rates of different levels. These results are discussed in the following sections.

3. Energy spectrum of ^{24}Ne

The band mixing calculations for obtaining the energies and the wavefunctions of different states of ^{24}Ne are performed in four parts. In the first stage the states of good angular momenta are projected from only the lowest oblate and prolate HF solutions. The projected spectra are displayed separately in part A of figure 2. It may be noted that even projection from a single intrinsic state (oblate or prolate) does not give a rotational spectrum. In the second stage of the calculations we mixed the states obtained in part A. The resulting spectrum is shown in part B of figure 2. The states in the spectrum B are widely displaced as compared to their positions in spectrum A. The displacement is mainly caused by

Table 3. Various intrinsic states of ^{24}Ne

State No.	Shape	Hole k	Particle k	Total K	Energy (MeV)
1	Oblate			0	−32·84
2	Oblate	5/2 p −5/2 p	3/2 p −3/2 p	0	−26·18
3	Prolate			0	−32·79
4	Prolate	5/2 n −5/2 n	1/2 n −1/2n	0	−29·68
5	Oblate	−1/2 n	−1/2′ n	0	−28·16
6	Oblate	−5/2 p	−1/2 p	2	−29·79
7	Prolate	−5/2 n	−1/2′ n	2	−30·45
8	Prolate	−1/2 p	3/2 p	2	−28·49
9	Prolate	−5/2 n	−1/2″ n	2	−28·30

the orthonormalization of the states and is only partly due to the mixing of the states by the Hamiltonian. The downward displacement of the lowest states with $J = 0, 2, 4$ is a measure of the mixing of the prolate and the oblate shapes by the Hamiltonian. As can be seen from figure 2B, this displacement is almost 0·5 MeV.

The third stage of the calculation consists of mixing the states projected from the oblate and the prolate HF states together with other $K = 0$ states listed in table 3. The resulting spectrum is shown in part C of figure 2. A comparison of spectra B and C shows that besides lowering all the states in spectrum C relative to those in spectrum B, this calculation has introduced many additional low-lying states. The comparison of spectrum C with the experimental spectrum F shows that except for the second $J = 2$ state, spectrum C agrees well with the experimental spectrum.

It may be recalled that similar calculations of Khadkikar *et al* (1971) using the renormalized interaction of Kuo could not give equally good results for these states and overall the spectrum was compressed. The reason for this disagreement lies mainly in the fact that the PW interaction, employed in our calculations, and the Kuo interaction are different mainly in their deformation producing properties. In fact it has been shown (Kulkarni and Pandya 1973) that the PW interaction gives less deformation as compared to the Kuo interaction. As a result the PW interaction decreases the moment of inertia and stretches the spectrum. At the same time the sequence of occupied orbitals is changed from k=1/2, 3/2, 1/2′ for Kuo interaction to k=1/2, 3/2, 5/2 for PW interaction for the lowest prolate HF solution. Thus the prolate HF solution is qualitatively different for the two interactions. This accounts for the fact that intermediary particle-hole excitations were absolutely essential (Khadkikar *et al* 1971) for mixing the prolate and oblate shapes with Kuo's interaction, while in the case of PW interaction the two shapes seem to mix even without introducing excitations. How-

ever, even after this mixing, the excited states are not obtained at low enough energies.

We note that K = 0 bands with particle-hole excitations play an important role in obtaining an energy spectrum in partial agreement with observations. However, one also sees that the second $J = 2$ state in spectrum C is even now about 1 MeV above the corresponding experimental state. This strongly emphasises the need for the inclusion of additional K = 2 bands. We therefore included the lowest K = 2 intrinsic states 6 and 7 listed in table 3. The final spectrum obtained using all these seven states is given in part D of figure 2. It is obvious that the inclusion of K = 2 bands has lowered the second $J = 2$ state appreciably. As a result spectrum D is in very good agreement with the experimental spectrum (Howard *et al* 1970). Spectrum D is also compared with the shell model spectrum (*see* spectrum E) obtained by Robertson *et al* (1973) using the same interaction. Though the absolute energy of the ground $J = 0$ state for the shell model calculation is 1·7 MeV lower than the one calculated here, the relative spacings are reproduced quite well. Finally, we have checked that when the additional intrinsic states 8 and 9 corresponding to K = 2 prolate bands are also included in the calculations, they neither improve the ground state energy nor affect the relative spacings appreciably, and therefore these results are not presented here. This perhaps indicates a rapid convergence or saturation of the configuration space as far as the energy spectrum calculation is concerned.

We now elucidate further the structure of the various levels in the ^{24}Ne spectrum by analysing the calculated wavefunctions in terms of different intrinsic states. One would like to know to what extent each of the configurations 1–7 are represented in the calculated wavefunctions. The overlaps of the normalized good angular momentum states projected from different configurations with the calculated eigenstates will give us the measure of the extent to which that configuration is present in different eigenstates. In table 4 we have given the overlaps of the states projected from seven configurations with the six low-lying calculated wavefunctions for $J = 0$, 2 and 4. However since the states projected from these configurations are not orthogonal, one needs to know their mutual overlaps in order to extract the complete information regarding the structure of these wavefunctions. Table 5 gives the overlaps of these normalized projected states.

Table 4. The overlaps of different bands with the calculated wavefunctions

J	E_J	1	2	3	4	5	6	7
0_1	−36·73	−0·934	0·638	−0·913	−0·204	0·267	0	0
0_2	−31·82	−0·079	0·168	−0·301	0·908	0·564	0	0
2_1	−34·73	−0·894	0·192	0·791	0·181	0·044	−0·543	−0·277
2_2	−32·73	−0·167	0·178	−0·382	−0·072	−0·601	0·564	−0·833
2_3	−31·24	−0·378	−0·033	−0·249	−0·468	0·219	0·374	0·405
4_1	−32·64	0·655	0·273	0·897	0·181	0·104	0·780	−0·315

Table 5. Some off-diagonal matrix elements of overlap matrices for the projected $J = 0$, 2 and 4 states. The pair of numbers in the bracket correspond to the intrinsic states as enumerated in table 3.

J	(12)	(13)	(14)	(15)	(16)	(17)	(23)
0	−0·524	0·828	0·058	−0·332	0	0	−0·654
2	−0·112	−0·517	−0·035	−0·108	0·247	0·249	0·154
4	0·230	0·411	0·038	0·269	0·434	−0·221	0·141
J	(24)	(25)	(26)	(27)	(34)	(35)	(36)
0	−0·035	0·402	0	0	0·012	−0·569	0
2	0·016	−0·084	0·082	−0·141	0·001	0·307	−0·750
4	−0·004	−0·141	0·498	0·016	−0·005	−0·135	0·624
J	(37)	(45)	(46)	(47)	(56)	(57)	(67)
0	0	0·234	0	0	0	0	0
2	−0·061	−0·142	−0·048	−0·027	−0·246	0·440	−0·105
4	−0·114	0·151	0·041	−0·092	−0·131	−0·364	−0·153

In the light of these results one can see that the ground state (0^+) can be described as prolate (oblate) HF-projected state with sizable correlations from the orthogonalized component of oblate (prolate) J-projected HF state. In addition there are small correlations from particle-hole excited states. The second 0^+ state, however, mainly consists of 1 particle-1 hole oblate and 2 particle–2 hole prolate states. The first excited 2^+ state has a structure similar to that of the ground 0^+ state but in addition there is a sizable contribution from $K = 2$ particle-hole excited states. The second 2^+ state and the 3^+ state mainly arise from $K = 2$ particle-hole excited " bands " while the third 2^+ state is spread over all the intrinsic states. The first 4^+ state arises from prolate (oblate) HF state and one $K = 2$ particle-hole excited state. These results are quite useful to understand the quadrupole electric transition rates between these levels as discussed in the next section.

4. Electric quadrupole transitions

The electric quadrupole moments and transition probabilities are calculated for the states of figure 2D. The effective charge used for proton is $1·5\,e$ and that for neutron is $0·5\,e$ in accordance with the usual practice in d–s shell calculations. The value of the oscillator parameter b used is 1·71 F. Table 6 shows the calculated BE2 values (in units of e^2F^4) along with the shell model values obtained using the same effective charges. It is observed that the calculated electric transition rates are somewhat higher than the shell model value. Also the charge quadrupole moment of the first $J = 2$ state is calculated to be $5·64\,eF^2$ whereas the

Table 6. The reduced electric quadrupole transition rates B(E2) in e^2F^4

Initial state	Final state	Calc.	Shell	Exp.
2_1	0_1	41·3	36·7	$26 \cdot 2^{+18 \cdot 0}_{-4 \cdot 5}$
2_2	0_1	2·5	2·0	
2_3	2_1	35·6	27·8	
4_1	2_1	39·6	30·4	
4_2	2_1	11·3	6·9	
0_2	2_1	8·1	1·4	
0_2	2_2	8·8	9·8	
4_1	2_2	0·25	..	

corresponding shell model value is 2 eF^2. This shows that even though the relative separation of the levels are reproduced quite well, the calculated wavefunctions are more collective than the corresponding shell model wavefunctions. We however expect that the inclusion of more and more states will reduce the collectivity of the calculated wavefunctions gradually. Unfortunately there is not much information available about the transition rates experimentally. The only piece of datum available regarding the value of the transition probability for $2_1 \rightarrow 0_1$, however, agrees well with the calculated one within experimental errors.

From the structure of the wavefunctions (*see* table 4) one sees that the states arising mainly from the same 'bands' have strong transition probabilities while the transition rate from second 0^+ to the first 2^+ state is small as the former arises from 2 particle–2 hole neutron excitations on the prolate HF state. This fact also qualitatively explains the large enhancement factor (1·92) for the excitation of the second 0^+ state over the 0^+ ground state in (t, p) reaction (Silbert and Jarmie 1961). One is tempted to draw an analogy with a pairing vibration though the collectivity is not very pronounced in the present case. The first 0^+, 2^+, 4^+ states have similar intrinsic structure and hence are connected by large reduced quadrupole transitions. On the other hand the second 2^+ state arises mainly from a $K = 2$ band and has significantly large transition rate to the first 2^+ state only, as this latter state also has a sizable contribution from the $K = 2$ band.

5. Conclusions

Band mixing calculations of ^{24}Ne based on particle-hole excitations on near-degenerate prolate and oblate HF states have yielded energy levels in good agreement with the experimental as well as the shell model spectra. However the calculated wavefunctions do not seem to agree well with the shell model wavefunctions as evidenced by the higher collectivity in the case of the electric quadrupole moments and transition rates. The inclusion of $K = 2$ bands and the choice of smaller-deformation-producing interaction are important factors in reproducing the energy levels of ^{24}Ne so well. One can also say that the shape mixing is enhanced

by the inclusion of K = 2 bands. It is doubtful if the results for energy spectrum resulting from band mixing calculations could be further improved by including more and more determinantal states. The choice of the number of determinantal states that should be included in the configuration space depends on how different the included intrinsic states are in their contents of states of good angular momenta. For example, mixing of states 8 and 9 did not make an appreciable change in the energy levels. Thus it seems that band mixing calculations can provide a good approximation to lengthy exact shell model calculations, and should be especially useful whenever the exact shell model calculations are not possible as in the fp shell. In addition they have the advantage of providing a useful physical insight into the structure of the observed nuclear states, and their interrelationship. For example we can understand the nature of the electric quadrupole transition rates and the enhancement factor in the (t,p) reaction for the excited 0^+ state in terms of the structure of the intrinsic states. This would become an even more important factor when one considers simultaneously the structure of a number of neighbouring nuclei and the systematics of their properties. We hope to discuss this point further in a separate publication.

References

Becker J A, Chase L F Jr, McDonald R E and Warburton E K 1968 *Phys. Rev.* **176** 1310
Halbert E C, McGrary J B, Wildenthal B H and Pandya S P 1971 *Advances in nuclear physics* Vol 4, ed M Baranger and E Vogt (Plenum Press, New York)
Howard A J, Hirko R G, Bromley D A, Bethge K and Olness J W 1970 *Phys. Rev.* **C1** 1446
Khadkikar S B, Nair S C K and Pandya S P 1971 *Phys. Lett.* **36B** 290
Kulkarni D R and Pandya S P 1973 *Pramāṇa* **1** 269
Kuo T T S 1967 *Nucl. Phys.* **A103** 71
Macferlane M H and Shukla A P 1971 *Phys. Lett.* **35B** 11
Preedom B M and Wildenthal B H 1972 *Phys. Rev.* **C6** 1633
Robertson R G H and Wildenthal B H 1973 Preprint, Michigan State University (MSUCL–80)
Silbert M G and Jarmie N 1961 *Phys. Rev.* **123** 221